Volume 1 | Number 1 | Jan 2013 | Pages 1–100

PCCP

Physical Chemistry Chemical Physics
www.rsc.org/pccp

ROYAL SOCIETY OF CHEMISTRY

ROYAL SOCIETY OF CHEMISTRY

www.rsc.org/pccp

TOC

Functionalized silicene with magnetic superhalogens has potential to be a magnetic half-metal.

Tuning Electronic and Magnetic Properties of Silicene with Magnetic Superhalogens

Tianshan Zhao,[†] Shunhong Zhang,[†] Qian Wang,[*†‡] Yoshiyuki Kawazoe,[§] and Puru Jena[‡]

[†]HEDPS, Center for Applied Physics and Technology, College of Engineering, Peking University, Beijing 100871, China

[‡]Department of Physics, Virginia Commonwealth University, Richmond, Virginia 23284, United States

[§]Institute for Material Research, Tohoku University, Sendai, 980-8577, Japan

ABSTRACT

Due to its compatibility with the well-developed Si-based semiconductor industry, silicene has attracted considerable attention. Using density functional theory we show for the first time that recently synthesized superhalogen $MnCl_3$ can be used to tune the electronic and magnetic properties of silicene, from semi-metallic to semiconducting with a wide range of band gaps, as well as from nonmagnetic to ferromagnetic (or antiferromagnetic) by changing the coverage of the superhalogen molecules. The electronic properties can be further modulated when a superhalogen and a halogen are used synergistically. The present study indicates that because of large electron affinity and rich structural diversity superhalogen molecules have advantages over the conventional halogen atoms in modulating material properties of silicene.

I. INTRODUCTION

In spite of the unique properties of graphene[1] and considerable efforts in the past decade to functionalize it for tailored applications, its limitations have spurred much interest in the search of alternate two-dimensional (2D) materials beyond graphene. Among these is silicene, a 2D allotrope of silicon, which can be easily integrated into the currently well-developed Si-based semiconductor industry. Following the theoretical prediction of its possible existence,[1-3] many experimental efforts have been devoted to the synthesis of silicene, and some significant progress has been reported.[4-6] Silicene has a buckled honeycomb structure. Due to strong spin orbit interaction, it has the potential to overcome limitations encountered in graphene, particularly the weak spin orbit interaction. In addition, quantum Hall effect and topological insulating states in silicene have been demonstrated.[7, 8] However, similar to graphene, pristine silicene is a gapless semiconductor[9, 10] and has a linear energy-momentum relationship in the vicinity of the Dirac point.[2, 5] Although the linear band dispersion gives rise to high carrier mobility, the absence of band gap hinders its practical application in building realistic nano-electronic devices. Inspired by extensive attempts to open the band gap in gapless graphene, similar strategies have been proposed to tailor the electronic structure of silicene, including introduction of local defect or Si adatoms,[11] applying external electric fields,[12, 13] chemical functionalization using hydrogenation[14-16] or halogenation,[17] and doping foreign atoms such as alkali metal,[18-20] or $3d$ transition metal atoms,[20, 21] or some other light atoms.[22]

In this work, we consider, for the first time, the use of magnetic superhalogen molecules instead of conventional halogen atoms to modulate the electronic structure as

well as magnetism of silicene. Superhalogens belong to an important family of superatoms[23] that possess electron affinity (EA) even larger than Cl, the element with the highest EA in the periodic table. Among all the studied superhalogens, Mn_xCl_y belongs to a unique class of magnetic family which has been recently studied theoretically[24, 25] and synthesized experimentally.[24] The high EA and intrinsic magnetism of Mn_xCl_y make this superhalogen family particularly desirable for functionalizing materials. We choose the $MnCl_3$[24] as a representative of magnetic superhalogens to functionalize silicene. We address the following questions: What is the preferable adsorption site of $MnCl_3$ on a silicene sheet? How do the geometry and electronic structure of silicene change with the coverage of $MnCl_3$? Can silicene be rendered magnetic with appropriate choice of ligands?

II. COMPUTATIONAL PROCEDURES

The atomic structure and electronic and magnetic properties are calculated using spin-polarized density-functional theory (DFT) and generalized gradient approximation (GGA)[26] for exchange and correlation potential as implemented in the Vienna *Ab initio* Simulation Package (VASP).[27] The projector-augmented wave (PAW) method[28] and Perdew-Burke-Ernzerhof (PBE) exchange correlation functional[26] are used. For all structural relaxations the convergence criteria for total energy and Hellmann-Feynman force is set at 10^{-4} eV and 10^{-2} eV/Å, respectively. The plane-wave cutoff energy is set to be 450 eV. The $3s^23p^2$, $3d^64s^1$, and $3s^23p^5$ electron orbitals are treated as valence states for Si, Mn and Cl, respectively. A 3×3 supercell with a vacuum space of 15 Å between the silicene sheets in the direction perpendicular to the plane is used in order to avoid

virtual interactions. The Brillouin zone is sampled by a 7×7×1 k-point grid within the Monkhorst-Pack scheme.[29] To study the thermodynamics of the adsorption of $MnCl_3$ on silicene sheet, we calculate the adsorption energy E_a, as

$$E_a = - (E_{total} - nE_{MnCl3} - E_{silicene})$$

where E_{total}, E_{MnCl3}, and $E_{silicene}$ are the total energies of $MnCl_3$ adsorbed silicene, $MnCl_3$ molecule, and pristine silicene, respectively. n is the number of $MnCl_3$ molecules. The parameter Δ used to measure the average buckling of silicene sheet upon surface decoration, is defined as,

$\Delta = 2$(sum of heights of top atoms – sum of heights of valley atoms)/total number of atoms.

III. RESULTS AND DISCUSSION

We begin with the total energy calculations of neutral $MnCl_3$ and pristine silicene to test our computational procedure. The lowest energy structure of neutral $MnCl_3$ is found to be same as that identified earlier by comparing experiment and theoretical calculations.[24] The ground state configuration of $MnCl_3$ has a planer geometry with C_{2v} symmetry with the Mn atom in the center and the three Cl atoms bonded to the Mn dissociatively. The calculated two different Mn-Cl bond lengths (2.14 Å and 2.16 Å, respectively), spin magnetic moment (4.0 μ_B) and EA (4.90 eV) of $MnCl_3$ are in good agreement with previous results.[24] For pristine silicene, the calculated lattice parameter, average buckling and average Si-Si bond length are 3.89, 0.49 and 2.29 Å, respectively, which compare well with the corresponding values of 3.83, 0.44 and 2.25 Å obtained in

a previous study.[2]

1. Modulation with MnCl₃ in low coverage

To determine the preferable adsorption site of MnCl₃ on silicene we considered six possible initial configurations in the 3×3 silicene supercell, as shown in Fig. 1. In configuration (a) MnCl₃ is introduced on the top site of a Si atom *via* formation of the Mn-Si bond. In configuration (b) MnCl₃ is placed on the hollow site of a hexagon where Cl bonds with Si. In configuration (c) MnCl₃ plane is vertical to silicene surface *via* the Cl-Si bonding where the Cl-Si bond is along the C_{2v} axis of MnCl₃. Configuration (d) is similar to configuration (c) except that the Cl atom bonded to silicene is not on the C_{2v} axis. In configuration (e), MnCl₃ penetrates into the sheet where the Mn atom is at the center of the hexagon. Finally, in configuration (f), the C_{2v} axis of MnCl₃ is vertical to silicene sheet with each of the two symmetrical Cl atoms bonded with a Si atom. Upon full geometry optimization, configurations (a), (b), and (f) converged to the same structure, as shown in Fig. 2(a), which is found to be the lowest energy configuration of the MnCl₃-adsorbed silicene. Configurations (c) and (d) are higher in energy by 0.43 and 0.56 eV, respectively, than the lowest energy structure. MnCl₃ dissociated in configuration (e) resulting in a much higher energy structure (1.31 eV). In the lowest energy configuration, we label the two different sub-lattices of silicene as sublattice "A" and "B", respectively, corresponding to the "top" and "valley" sites marked in previous work.[20] The Mn atom becomes 4-fold coordinated and the planar structure of MnCl₃ is deformed due to the chemical bonding between Mn-Si and Cl-Si. The average buckling of the MnCl₃-

adsorbed silicene is 0.53 Å, which is slightly larger than 0.49 Å in pristine silicene. The average Si-Si bond length (2.33 Å) is also slightly longer than that of pristine sheet (2.29 Å). The Si-Mn bond length is 2.67 Å. The average Cl-Si and Cl-Mn bond lengths are 2.23 and 2.20 Å, respectively. Our calculated adsorption energy of MnCl$_3$ on silicene is 1.34 eV, which is larger than that of Cl or Si to silicene (1.018 eV and 0.03 eV, respectively),[30,11] but smaller than that of F to silicene (1.982 eV).[30] The calculated results are listed in Table 1.
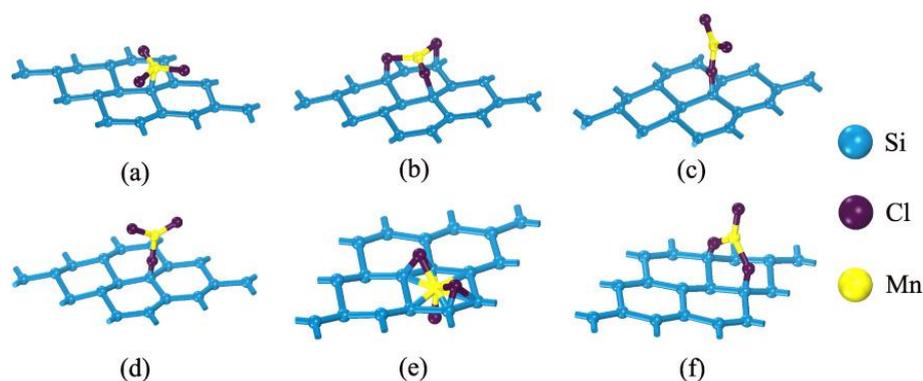

Fig. 1   Six initial configurations of MnCl$_3$-adsorbed silicene in the 3×3 supercell.

To study the effect of MnCl$_3$ adsorption on the electronic structure of silicene, we calculated the electronic band structure and partial density of state (PDOS). The results are given in Fig. 3 (a). The band structure shows that the spin up channel exhibits metallic behavior as a partially occupied band crosses the Fermi level in between the M and K points in the Brillouin Zone, while the spin down channel exhibits semiconducting feature with a direct band gap of 0.28 eV at the Γ point, suggesting that the MnCl$_3$-adsorbed

silicene is half-metallic. From the PDOS we see that the electronic states near the Fermi level are mainly located in the spin up channel and contributed by the Si $3p$ and Mn $3d$ orbitals. The conduction bands in the spin up channel are dominated by the Si $3p$ orbitals while the valance bands are mainly contributed by the Si $3p$ and Mn $3d$ orbitals. In contrast, in the spin down channel the valance bands are dominated by the Si $3p$ orbitals while the conduction bands are mainly contributed by the Mn $3d$ and Si $3p$ orbitals. Therefore, we conclude that the adsorption of $MnCl_3$ opens the band gap in the spin down channel while making the spin up channel metallic, thus transforming silicene from a gapless semiconductor to a half-metal.
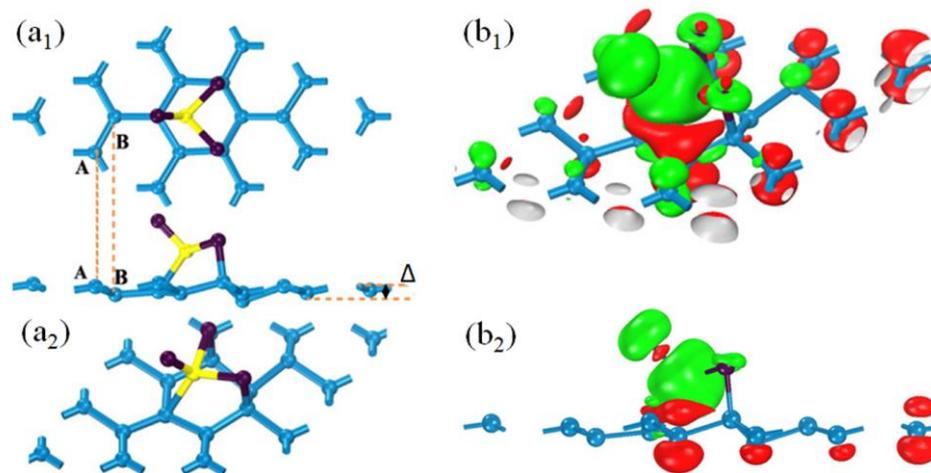

Fig. 2 (a_1) Top and side views, and (a_2) perspective view of the geometry of $MnCl_3$-adsorbed silicene. (b_1) and (b_2) Corresponding spin density isosurfaces with a value of 0.01 e/Å^3 in different views. Green and red isosurfaces represent spin-up and spin-down charges, respectively.

Since isolated $MnCl_3$ is intrinsically magnetic we now study the effect of its adsorption on the spin polarization of the silicene substrate. The magnetic

moment/supercell is found to be of 4.00 μ_B and mostly localized on the Mn site which carries a magnetic moment of 4.03 μ_B. The three Cl atoms are polarized ferromagnetically, but with very small magnetic moment of 0.01, 0.01, and 0.12 μ_B, respectively. The Si atom bonded with the Mn is polarized antiferromagnetically with a magnetic moment of -0.07 μ_B, while the neighboring Si atoms are aligned ferromagnetically to Mn with magnetic moments of 0.03, 0.02 and 0.02 μ_B, respectively. The Si sites neighboring to the two Si atoms bonded with the Cl atoms, are polarized antiferromagnetically. To visualize this complicated spin polarization, the spin density isosurfaces are plotted in Fig. 2 (b). The net polarization of the substrate is antiferromagnetic (AFM). Thus, we see that the adsorption of the superhalogen converts silicene sheet from a gapless semiconductor to a magnetic half-metal.
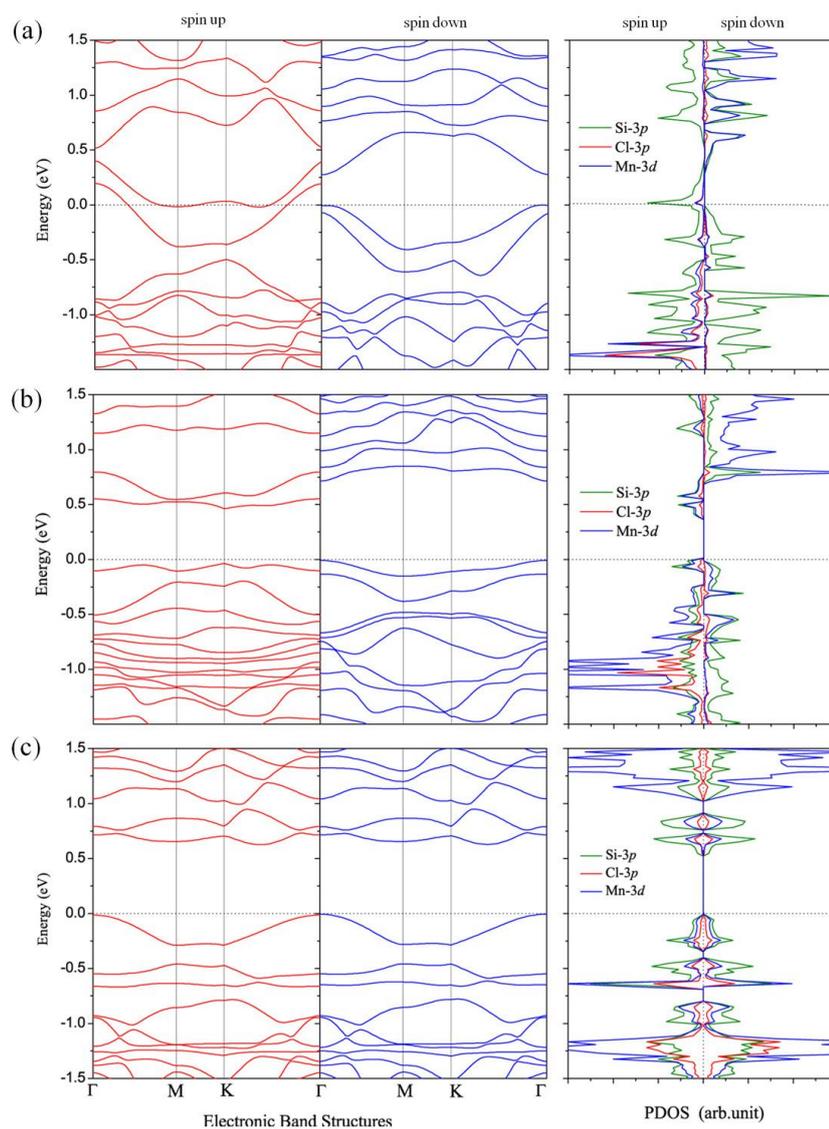
Fig. 3 Spin-polarized band structure and PDOS of (a) MnCl$_3$-adsorbed silicene, (b) the 2MnCl$_3$-silicene-SS, and (c) the 2MnCl$_3$-silicene-OS. The high symmetry K point paths are Γ (0, 0) - M (1/2, 0) - K (1/3, 1/3) - Γ (0, 0). The Fermi level is at 0.00 eV.

2. Effect of MnCl$_3$ coverage

To study the effect of supercell on the electronic and magnetic properties of silicene we considered the adsorption of one MnCl$_3$ and enlarged the supercell from 3×3 to 4×4, 5×5 and 6×6. The calculated results show that the morphology of the MnCl$_3$ adsorbed

9 / 22

silicene remains unchanged, as shown in Fig. 4 (a,b,c). Following the same procedure as above, we calculated the electronic and magnetic properties of the MnCl₃-adsorbed silicene using these enlarged supercells. The calculated band structures and DOSs are quite similar to Fig. 3(a) showing half-metallic feature with 0.00 eV band gap. In addition, the calculated total magnetic moment/supercell is still 4.00 μ_B at low coverage. The results are summarized in Table 1 and the spin density isosurfaces are plotted in Fig.4 (e,f,g), showing that a 3×3 supercell is adequate to mimic the adsorption of the MnCl₃ on silicene sheet.
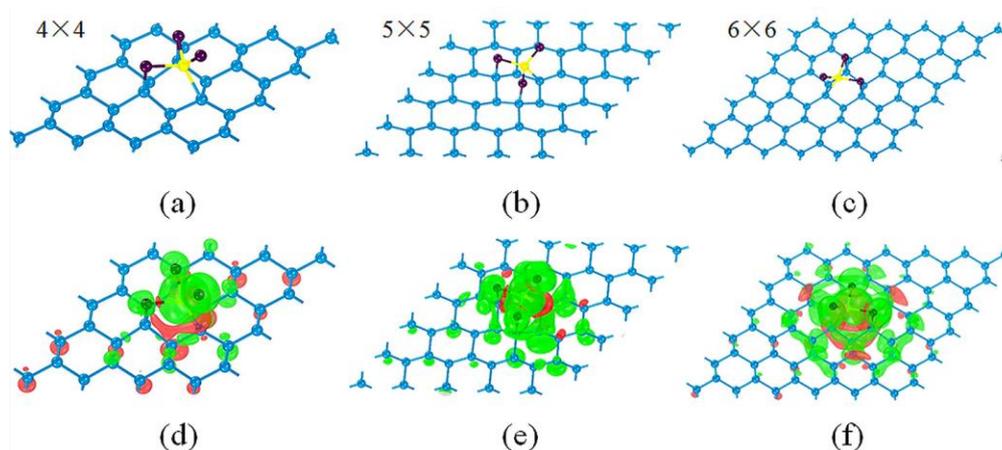

Fig. 4 (a-c) Perspective view of the geometry of MnCl₃-adsorbed silicene in 4×4, 5×5, and 6×6 supercells. (d-f) Corresponding spin charge density isosurfaces with an isovalue of 0.01 e/Å³. Green and red isosurfaces represent the spin-up and spin-down charges, respectively.

For the higher coverage case involving two MnCl₃ molecules we then considered the 3×3 silicene supercell. We first introduced two superhalogen molecules on the same side of silicene. Due to the C_{2v} symmetry of MnCl₃, different adsorption sites of the

superhalogens and their different relative orientations result in different adsorption configurations. We, therefore, carried out extensive search for the lowest energy configuration of the two-MnCl$_3$-adsorbed silicene system with full geometry optimization. The initial adsorption configurations are provided in Fig. S2. We term this system as 2MnCl$_3$-Silience-SS, where "SS" means the two superhalogens are adsorbed on *Same Side* of the silicene sheet. The lowest energy configuration is plotted in Fig. 5 (a), where the average bond lengths of Mn-Si, Cl-Si, and Mn-Cl are 2.50, 2.45 and 2.20 Å, respectively. The average bond length of Si-Si remains unchanged. The average buckling and adsorption energy per superhalogen are calculated to be 0.58 Å and 1.42 eV, which are larger than those of the single MnCl$_3$-adsorbed case by 0.05 Å and 0.07 eV, respectively. This is due to the change in the electronic structure of silicene substrate following the adsorption of the first MnCl$_3$ moiety, consequently resulting in a stronger binding for the second adsorbate.

The calculated electronic band structure is plotted in Fig. 3 (b), which shows that the adsorption of two MnCl$_3$ superhalogens opens the band gap of silicene in both the spin up and spin down channels forming an indirect band gap semiconductor with a gap of 0.42 eV (the gap of spin up channel is 0.72 eV, while that of spin down channel is 0.44 eV). The PDOS shows that the electronic states in the valance bands near the Fermi level are mainly contributed by the Si 3p and Mn 3d orbitals with a small contribution from the Cl 3p orbitals. Si 3p orbitals shift down below the Fermi level as superhalogens draw electrons from silicene. In fact, charge analysis suggests that there are 0.61 electrons transferred from Si 3p_z orbitals of the substrate to the Cl 3p_z of the MnCl$_3$.
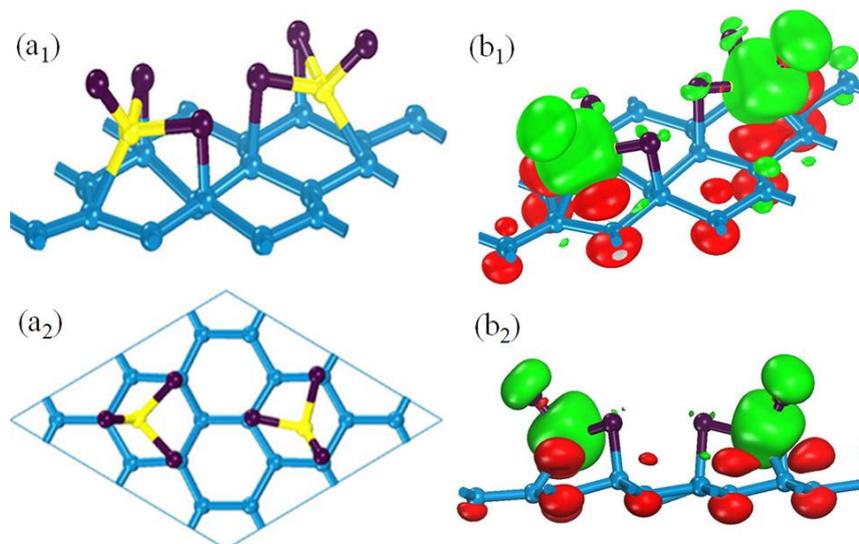
Fig. 5 (a_1) Side and (a_2) top views of the optimized geometry of $2MnCl_3$-Silicene-SS. (b_1) and (b_2) Corresponding spin density isosurface with a value of 0.01 e/$Å^3$ viewed from different directions. Green and red isosurfaces represent the spin-up and spin-down charges, respectively.

To study the magnetic coupling between the Mn atoms in $MnCl_3$ supported on silicene, we calculated the energy difference E_{ex} between the ferromagnetic (FM) and AFM coupling configurations, which is defined as $E_{ex} = E_{AFM} - E_{FM}$. The FM state is found be to be 20 meV lower in energy than the AFM state. The total moment of the $2MnCl_3$-Silicene-SS configuration is 8 μ_B of which magnetic moments of 3.89 μ_B and 3.96 μ_B are carried by the two Mn atoms. The Cl atoms are polarized ferromagnetically to the Mn atoms with each Cl atom carrying a magnetic moment of about 0.06 μ_B. The Si atoms on the substrate are mainly antiferromagnetically polarized, as visualized in Fig. 5 (b).

We then study the adsorption of two $MnCl_3$ moieties placed on opposite sides of silicene. There are also many possible adsorption configurations. We have tried 13 different configurations to search for the lowest energy structure, as shown in Fig. S3.

After full geometry optimization for each configuration, the lowest energy structure is found where the two superhalogens occupy a same hexagon of silicene with different orientations, as shown in Fig. 6 (a). Accordingly, we term this system as 2MnCl$_3$-Silicene-OS, where "OS" means the two superhalogens adsorbed on the *Opposite Sides* of silicene. The average bond lengths of the Si-Si, Mn-Si, Cl-Si, and Mn-Cl are 2.31, 2.45, 2.31, and 2.20 Å, respectively. The average buckling parameter, Δ of the 2MnCl$_3$-Silicene-OS is 0.51 Å. The adsorption energy is calculated to be 3.92 eV, which is 1.09 eV lower than the configuration where the two MnCl$_3$ superhalogens are adsorbed on the same side of silicene indicating that the two superhalogen molecules prefer to occupy the hollow site of a hexagon respectively on opposite sides of silicene in the supercell.

The calculated band structure reveals that the 2MnCl$_3$-silicene-OS is an indirect band gap semiconductor as the valence band maximum (VBM) is located at the Γ point while the conduction band minimum (CBM) is at the K point in the Brillouin zone (BZ), as shown in Fig. 3 (c). The calculated band gap is 0.63 eV. From the PDOS we see that the electronic states in the spin up and spin down channels are nearly symmetric, and the conduction bands and valence bands closing to the Fermi level are mainly contributed by Si $3p$ and Mn $3d$ orbitals with small contributions from Cl $3p$, while the others located further from the Fermi level are primarily contributed by the Mn $3d$ orbitals with small contributions from Si $3p$ and Cl $3p$ orbitals. The total energy calculations suggests that the magnetic coupling between the two Mn atoms is AFM which is 100 meV lower in energy than the FM configuration. The corresponding spin density distribution is plotted in Fig. 6 (b).
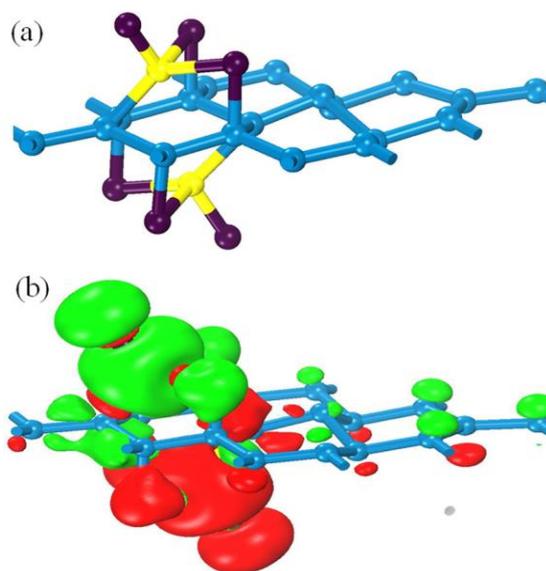
Fig. 6 (a) Geometry and (b) spin density isosurface with a value of 0.01 e/Å^3 of the 2MnCl$_3$-Silience-OS. Green and red isosurfaces represent the spin up and spin down charges, respectively.

3. Hybrid modulation with MnCl$_3$ and Cl

In this section we focus on modulating the properties of silicene by functionalizing it simultaneously with a superhalogen (MnCl$_3$) and a halogen (Cl). Starting with the preferable configuration of a single MnCl$_3$ adsorbed silicene, as shown in Fig. 2 (a), we introduced a Cl atom into the supercell at ten different nonequivalent sites on the same side where the superhalogen resides. These hybrid adsorption configurations are given in Fig. S4. The most preferable configuration, determined upon full geometry optimization of all the configurations, is given in Fig. 7 (a). The average Si-Si, Mn-Si, Cl-Si, and Mn-Cl bond lengths are 2.29, 2.63, 2.23, and 2.21 Å, respectively. The buckling parameter, Δ is found to be 0.53 Å, indicating that the effect of adding a Cl atom to the system on its geometry is subtle. However, band structure and total energy calculations show that the

electronic and magnetic properties are substantially affected by introducing a Cl atom to the system. The electronic band structure in Fig. 8 (a) shows that the hybrid structure with superhalogen and halogen co-adsorbed on silicene is an indirect band gap semiconductor with a gap of 0.25 eV. The band gap of spin-up channel is 0.62 eV while that of the spin-down channel is 0.56 eV, indicating that the hybrid system changes to a semiconductor from a half-metal of the superhalogen-adsorbed silicene. In addition, co-adsorption of halogen and superhalogen makes the substrate antiferromagnetically polarized. The Mn atom carries a magnetic moment of 4.04 μ_B and its two neighboring Cl atoms bonded to the substrate in $MnCl_3$ are polarized antiferromagnetically, while the other neighboring Cl is coupled ferromagnetically to Mn, leading to a total moment of 3 μ_B/supercell. The magnetic moment on the isolated Cl is -0.03 μ_B, which is also polarized anti-ferromagnetically. The isosurface of the spin density distribution is plotted in Fig. 7 (a_2).
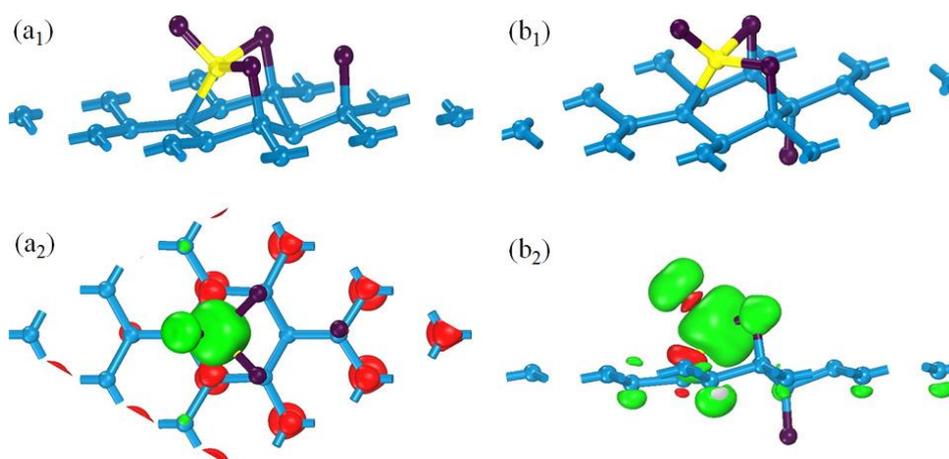

Fig. 7 (a_1) and (b_1) Geometries, and (a_2) and (b_2) spin density isosurfaces with a value of 0.01 e/Å^3 of $MnCl_3$ and Cl co-adsorbed silicene with the Cl atom on the same side and the opposite side of $MnCl_3$, respectively. Green and red isosurfaces represent the spin up and spin down charge, respectively.

We then introduced a Cl atom on the opposite side of $MnCl_3$. We again generated ten nonequivalent configurations as shown in Fig. S5. The most preferable configuration is plotted in Fig. 7 (b_1). The average Si-Si, Mn-Si, Cl-Si, and Mn-Cl bond lengths are calculated to be 2.29 Å, 2.63 Å, 2.23 Å, and 2.16 Å, respectively. The buckling parameter, Δ is 0.53 Å, showing once again that Cl does not have much influence on the geometry once silicene is decorated with $MnCl_3$ superhalogen. Compared to the configuration where Cl is adsorbed on the same side, this configuration is 0.57 eV lower in energy, suggesting that the halogen and superhalogen prefer to occupy opposite sides of silicene. Different from the configuration with both Cl and $MnCl_3$ on the same side, the Mn atom carries a magnetic moment of 4.39 μ_B and the three neighboring Cl atoms are polarized ferromagnetically. Some of the Si atoms in the substrate are also polarized ferromagnetically, as shown in Fig. 7 (b_2), leading to a total magnetic moment of 5 μ_B/supercell. The calculated band structure indicates that this system has a narrow direct band gap of 0.02 eV, as shown Fig. 8 (b), although both the spin-up and spin-down channels have a band gap of 0.22 eV. This system can be viewed as a novel quasi-spin-gapless semiconductor[9, 10] in which the valance electrons in the spin up channel can be easily excited into the spin down channel.
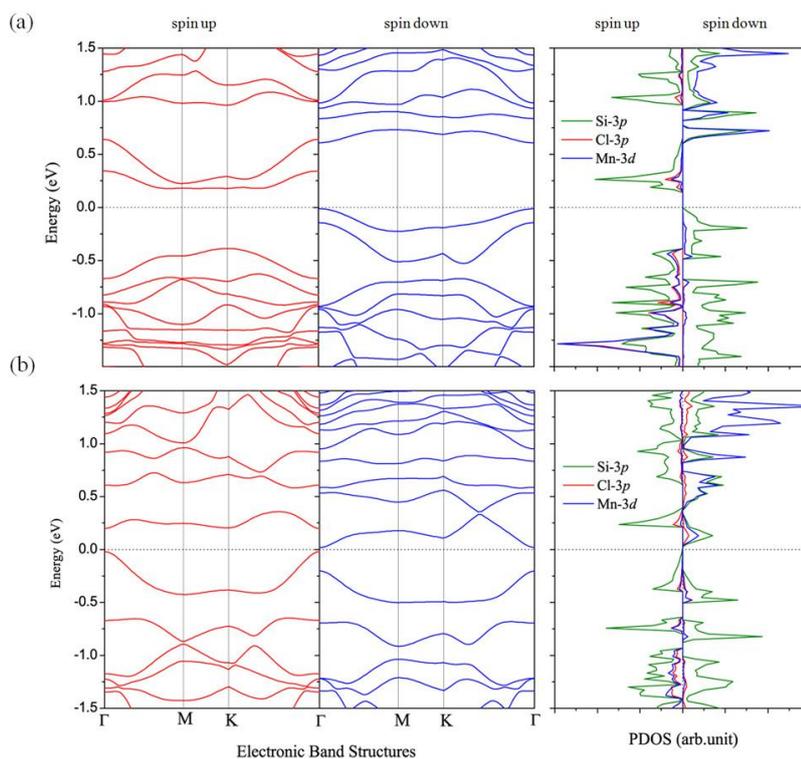
Fig. 8 Spin-polarized band structure and PDOS of the MnCl₃ and Cl co-adsorbed silicene with the Cl atom on the same side (a) and opposite sides (b) of MnCl₃.

IV. SUMMARY

Halogens, including F, Cl, Br, I and At, exhibit high electron affinities, superior chemical reactivity and strong oxidizing properties. The extensive use of halogens to materials synthesis and modification led us to explore functionalization of materials using superhalogens, which display even larger electron affinity, richer structural diversity, as well as novel properties as compared to halogens. In this study, for the first time, we have investigated functionalization of silicene using a magnetic superhalogen, namely, MnCl₃ which has been synthesized recently. From the results in Table 1 the following conclusions can be drawn: (1) MnCl₃ prefers to occupy the hollow site of silicene where

the Mn atom and two Cl atoms are bonded with the substrate, resulting in a 4-coordinated configuration for Mn. (2) When two $MnCl_3$ molecules are introduced to silicene, they prefer to reside on opposite sides. Similar is the case when $MnCl_3$ and one Cl are co-adsorbed. (3) The electronic properties and band gap of silicene can be tuned by varying the concentration of $MnCl_3$ as well as by simultaneous functionalizing with $MnCl_3$ and Cl. For example, with a single $MnCl_3$, functionalized silicene can be tuned from a gapless semiconductor to a half-metal, with two $MnCl_3$ molecules to an indirect band gap semiconductor, and finally back to quasi-spin-gapless semiconductor by introducing one $MnCl_3$ molecule and one Cl atom. The band gap changes over a wide range from 0.02 to 0.63 eV, depending on the concentration and the dopant. (4) Once the first $MnCl_3$ is adsorbed, it changes the electronic structure of the substrate and results in a stronger binding for the second adsorbate. (5) Magnetism shows complicated behavior: In an isolated state $MnCl_3$ has a magnetic moment of 4 μ_B. When one $MnCl_3$ is incorporated to a supercell, the total moment of the supercell remains 4 μ_B. This can be changed to 3 or 5 μ_B if a Cl atom is introduced on the same side or on the opposite side of $MnCl_3$. When two $MnCl_3$ superhalogens are adsorbed on the same side, the coupling between Mn atoms is FM, resulting a total moment of 8 μ_B/supercell. However, the coupling becomes AFM when the two superhalogens reside on opposite sides. The induced polarization of silicene also sensitively depends on the concentration and the identity of the adsorbates, providing additional freedoms for tuning the structure and properties of silicene. We hope that our theoretical study can motivate experimentalists to use superhalogens to functionalize silicene.

Table 1. Comparison of Si-Si, Mn-Si, Cl-Si, and Mn-Cl bond lengths (in Å), average buckling parameter, Δ (in Å), adsorption energy E_a (in eV), band gap E_g (in eV), and magnetic moment M /supercell (in μ_B) for different coverage and configurations. S and D stand for a single and two $MnCl_3$ superhalogens in the supercells, T represents one $MnCl_3$ and one Cl atom in the supercell, the superscripts 1 and 2 stand for adsorption on same side and opposite sides, respectively.

Configurations		Si-Si	Mn-Si	Cl-Si	Mn-Cl	Δ	E_a	E_g	M
I	silicene	2.29	-	-	-	0.49		0.00	0.00
II	$S_{(3\times3)}$	2.33	2.67	2.23	2.20	0.53	-1.34	0.00	4.00
III	$S_{(4\times4)}$	2.31	2.62	2.25	2.20	0.53	-1.46	0.00	4.00
IV	$S_{(5\times5)}$	2.29	2.60	2.26	2.20	0.50	-1.53	0.00	4.00
V	$S_{(6\times6)}$	2.29	2.55	2.26	2.20	0.50	-1.61	0.00	4.00
VI	$D^1_{(3\times3)}$	2.29	2.50	2.45	2.20	0.58	-2.83	0.28	8.00
VII	$D^2_{(3\times3)}$	2.30	2.45	2.31	2.20	0.51	-3.92	0.63	0.00
VIII	$T^1_{(3\times3)}$	2.29	2.63	2.23	2.21	0.53	-3.48	0.25	3.00
IX	$T^2_{(3\times3)}$	2.29	2.63	2.23	2.16	0.52	-4.05	0.02	5.00

AUTHOR INFORMATION

*E-mail: qianwang2@pku.edu.cn

ACKNOWLEDGMENTS

REFERENCES

1.   K. Takeda and K. Shiraishi, *Phys. Rev. B*, 1994, **50**, 14916-14922.

2.   S. Cahangirov, M. Topsakal, E. Aktürk, H. Şahin and S. Ciraci, *Phys. Rev. Lett.*, 2009, **102**, 236804.

3.   G. G. Guzmán-Verri and L. C. Lew Yan Voon, *Phys. Rev. B*, 2007, **76**, 075131.

4.   A. Fleurence, R. Friedlein, T. Ozaki, H. Kawai, Y. Wang and Y. Yamada-Takamura, *Phys. Rev. Lett.*, 2012, **108**, 245501.

5.   L. Chen, C.-C. Liu, B. Feng, X. He, P. Cheng, Z. Ding, S. Meng, Y. Yao and K. Wu, *Phys. Rev. Lett.*, 2012, **109**, 056804.

6.   B. Lalmi, H. Oughaddou, H. Enriquez, A. Kara, S. Vizzini, B. Ealet and B. Aufray, *Appl. Phys. Lett.*, 2010, **97**, 223109-223102.

7.   C.-C. Liu, W. Feng and Y. Yao, *Phys. Rev. Lett.*, 2011, **107**.

8.   X.-L. Zhang, L.-F. Liu and W.-M. Liu, *Sci. Rep.*, 2013, **3**.

9.   X. L. Wang, *Phys. Rev. Lett.*, 2008, **100**, 156404.

10.   X.-L. Wang, S. X. Dou and C. Zhang, *NPG Asia Mater*, 2010, **2**, 31-38.

11.   J. Gao, J. Zhang, H. Liu, Q. Zhang and J. Zhao, *Nanoscale*, 2013, **5**, 9785-9792.

12.   Z. Ni, Q. Liu, K. Tang, J. Zheng, J. Zhou, R. Qin, Z. Gao, D. Yu and J. Lu, *Nano Lett.*, 2011, **12**, 113-118.

13.   N. D. Drummond, V. Zólyomi and V. I. Fal'ko, *Phys. Rev. B*, 2012, **85**, 075423.

14.   Y. Ding and Y. Wang, *Appl. Phys. Lett.*, 2012, **100**, 083102.

15.   M. Houssa, E. Scalise, K. Sankaran, G. Pourtois, V. V. Afanas'ev and A. Stesmans, *Appl. Phys. Lett.*, 2011, **98**, 223107-223103.

16.   G. G. Guzmán-Verri and L. C. L. Y. Voon, *J. Phys. Condens. Matter*, 2011, **23**, 145502.

17.   F.-b. Z. Zheng, C.-w., *Nanoscale Res. Lett.*, 2012, **7**, 422.

18.   G. A. Tritsaris, E. Kaxiras, S. Meng and E. Wang, *Nano Lett.*, 2013, **13**, 2258-2263.

19.   R. Quhe, R. Fei, Q. Liu, J. Zheng, H. Li, C. Xu, Z. Ni, Y. Wang, D. Yu, Z. Gao and J. Lu, *Sci. Rep.*, 2012, **2**.

20.   H. Sahin and F. M. Peeters, *Phys. Rev. B*, 2013, **87**, 085423.

21.   X. Lin and J. Ni, *Phys. Rev. B*, 2012, **86**, 075440.

22.   J. Sivek, H. Sahin, B. Partoens and F. M. Peeters, *Phys. Rev. B*, 2013, **87**, 085444.

23.   P. Jena, *J. Phys. Chem. Lett.*, 2013, **4**, 1432-1442.

24.   M. M. Wu, H. Wang, Y. J. Ko, Q. Wang, Q. Sun, B. Kiran, A. K. Kandalam, K. H. Bowen and P. Jena, *Angew Chem Int Ed Engl*, 2011, **50**, 2568-2572.

25.   Y. Li, S. Zhang, Q. Wang and P. Jena, *J. Chem. Phys.*, 2013, **138**, 054309.

26.   J. P. Perdew, K. Burke and M. Ernzerhof, *Phys. Rev. Lett.*, 1996, **77**, 3865-3868.

27.   G. Kresse and J. Furthmüller, *Phys. Rev. B*, 1996, **54**, 11169-11186.

28.   P. E. Blöchl, *Phys. Rev. B*, 1994, **50**, 17953-17979.

29.   H. J. Monkhorst and J. D. Pack, *Phys. Rev. B*, 1976, **13**, 5188-5192.

30.   N. Gao, W. T. Zheng and Q. Jiang, *Phys. Chem. Chem. Phys.*, 2012, **14**, 257-261.